




GAS41 mediates proliferation and *GEM* chemoresistance via H2A.Z.2 and Notch1 in pancreatic cancer

Shilong Han^{1,2} · Chuanwu Cao^{1,2} · Rui Liu³ · YiFeng Yuan^{1,2} · Long Pan^{1,2} · Minjie Xu^{1,2} · Chao Hu^{1,2} · Xiaojun Zhang^{1,2} · Maoquan Li^{1,2} · Xiaoping Zhang^{1,2} 

Accepted: 11 April 2022 / Published online: 3 May 2022
© Springer Nature Switzerland AG 2022

Abstract

Purpose GAS41 is a YEATS domain protein that binds to acetylated histone H3 to promote the chromatin deposition of H2A.Z in non-small cell lung cancer. The role of GAS41 in pancreatic cancer is still unknown. Here, we aimed to reveal this role.

Methods GAS41 expression in pancreatic cancer tissues and cell lines was examined using qRT-PCR, Western blotting and immunohistochemistry. MTT, colony formation, spheroid formation and *in vivo* tumorigenesis assays were performed to assess the proliferation, tumorigenesis, stemness and gemcitabine (*GEM*) resistance of pancreatic cancer cells. Mechanistically, co-immunoprecipitation (co-IP) and chromatin immunoprecipitation (ChIP) assays were used to evaluate the roles of GAS41, H2A.Z.2 and Notch1 in pancreatic cancer.

Results We found that GAS41 is overexpressed in human pancreatic cancer tissues and cell lines, and that its expression increases following the acquisition of *GEM* resistance. We also found that GAS41 up-regulates Notch, as well as pancreatic cancer cell stemness and *GEM* resistance *in vitro* and *in vivo*. We show that GAS41 binds to H2A.Z.2 and activates Notch and its downstream mediators, thereby regulating stemness and drug resistance. Depletion of GAS41 or H2A.Z.2 was found to down-regulate Notch and to sensitize pancreatic cancer cells to *GEM*.

Conclusion Our data indicate that GAS41 mediates proliferation and *GEM* resistance in pancreatic cancer cells via H2A.Z.2 and Notch1.

Keywords Pancreatic cancer · Chemoresistance · GAS41 · H2A.Z.2 · Notch1

Shilong Han, Chuanwu Cao, Rui Liu and YiFeng Yuan Equally contributed to this work.

✉ Maoquan Li
cjr.limaoquan@vip.163.com

✉ Xiaoping Zhang
zxpky@126.com

¹ Department of Intervention and Vascular Surgery, Shanghai Tenth People's Hospital, Tongji University School of Medicine, 50 Chifeng Road, Yangpu, Shanghai 200072, China

² National Center Clinical Research for Interventional Medicine, Shanghai Tenth People's Hospital, 50 Chifeng Road, Yangpu, Shanghai 200072, China

³ Shanghai Tenth People's Hospital of Tongji University, Tongji University Cancer Center, Shanghai 200072, China

1 Introduction

Pancreatic cancer is a very aggressive malignancy with a 5-year overall survival rate of 11% [1]. It is the third leading cause of cancer-related mortality in men and women combined [2, 3]. Gemcitabine (*GEM*) alone or in combination with other traditional chemotherapeutic drugs such as nab-paclitaxel or oxaliplatin serves as the first-line chemotherapy for pancreatic cancer [4]. However, its survival benefits are rather modest, in part due to the rapid development of chemoresistance in initially sensitive tumors [5, 6]. Although established chemotherapeutic agents such as FOLFIRINOX and novel kinase inhibitors including Erlotinib and Refametinib are showing promise in reducing the growth of pancreatic cancer cells [7, 8], there remains an unmet clinical need in the treatment of pancreatic cancer. Cancer stem cells (CSCs) are well known for their resistance to therapy. Drug-induced pressure on tumor cells can

result in an enrichment of CSCs and/or force differentiated tumor cells to undergo phenotypic transition to a stem-like cell state, thereby conferring drug resistance [9]. Indeed, chemoresistance is often associated with activation of

CSC-specific pathways such as the NOTCH pathway [10, 11]. In particular, it has been reported that the NOTCH pathway drives the selective growth of stem-like, *GEM*-resistant (GR) pancreatic cancer cells [12]. However, the

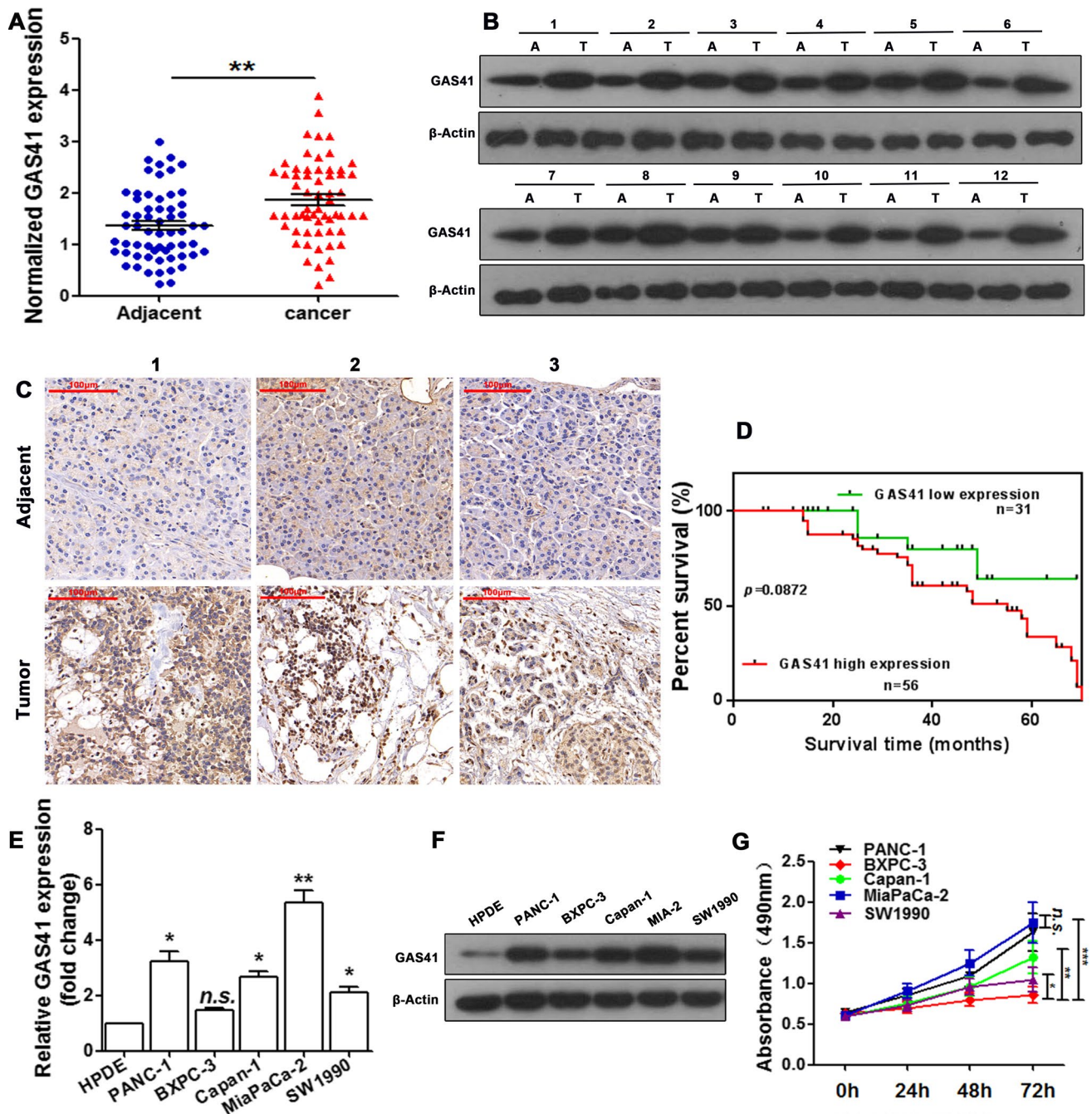


Fig. 1 GAS41 is overexpressed in human pancreatic cancer tissues and cell lines. (A–C) GAS41 expression in human pancreatic cancer and adjacent normal tissues evaluated by qRT-PCR (A; n = 87, $**p < 0.01$) and Western blotting (B; n = 12, A = adjacent, T = tumor), and IHC (C, Scale bars = 100 μ m). (D) Kaplan-Meier survival curves of pancreatic cancer patients with low (n = 31) or high (n = 56) GAS41 expression. (E, F) GAS41 expression in human pancreatic cancer cell lines (PANC-1, BXPC3, Capan-1, MiaPaCa-2 and

SW1990) and a normal pancreatic duct epithelial cell line (HPDE) assessed by qRT-PCR (E) and Western blotting (F). n = 3; $*p < 0.05$, $**p < 0.01$ vs. HPDE; n.s. = no significant difference vs. HPDE. (G) Growth curves of human pancreatic cells (PANC-1, BXPC3, Capan-1, MiaPaCa-2 and SW1990) grown in the presence of 2 μ M *GEM* measured by a MTT assay. n = 3, $*p < 0.05$, $**p < 0.01$, $***p < 0.001$, n.s. = no significant difference

molecular mechanisms that lead to NOTCH activation in these cells remain poorly understood.

Histone variants are known to play fundamental roles in chromosome segregation and gene expression. H2A.Z, a member of the H2A histone variant family, has been reported to regulate stem cell homeostasis and cancer development [13]. H2A.Z can either enhance or repress gene transcription, and the transcriptional output is controlled by post-translational modifications, most notably acetylation [13, 14]. In particular, chromatin deposition of acetylated H2A.Z has been linked to the activation of Notch [15]. There are two isoforms of H2A.Z, known as H2A.Z.1 and H2A.Z.2 [16]. Of these two, the H2A.Z.2 isoform has been shown to promote drug resistance in malignant melanoma [17]. Based on these findings, we hypothesized that acetylated H2A.Z.2 (acH2A.Z.2) may drive Notch activation and *GEM* resistance in pancreatic cancer.

The YEATS domain is a protein module that binds to acetylated histones. Glioma amplified sequence 41 (GAS41, YEATS4), a human YEATS-domain containing protein, is a component of chromatin-modifying complexes responsible for the deposition of H2A.Z onto chromatin [18, 19]. Although the significance of GAS41 in human cancer is still largely unexplored, a recent study has shown that GAS41 may drive non-small cell lung cancer (NSCLC) development by binding to acetylated histone H3 to promote the chromatin deposition of H2A.Z [20]. Another recent study has shown that mutations in GAS41 are associated with dysregulated H2A.Z deposition in uterine leiomyoma, a disease that has been associated with increased Notch expression and activation [21, 22]. Thus, GAS41, by controlling H2A.Z deposition, may be a novel regulator of Notch signaling [15, 18, 19]. Here, we evaluated the role of GAS41 in pancreatic cancer, with a focus on the acquisition of *GEM* resistance. We found that GAS41 expression is increased in human pancreatic cancer tissues and cell lines, and further increases following the acquisition of resistance. In addition, we found that GAS41 binds to acH2A.Z.2 and leads to up-regulation of Notch and its downstream mediators that regulate stemness and resistance. Overexpression of GAS41 or H2A.Z.2 was found to increase Notch expression and resistance to *GEM*, while GAS41 or H2A.Z.2 silencing down-regulated Notch and sensitized pancreatic cancer cells to *GEM* *in vitro* and in an *in vivo* xenograft mouse model. Our findings suggest that GAS41 may serve as a promising target to promote chemosensitivity in pancreatic cancer.

2 Materials and methods

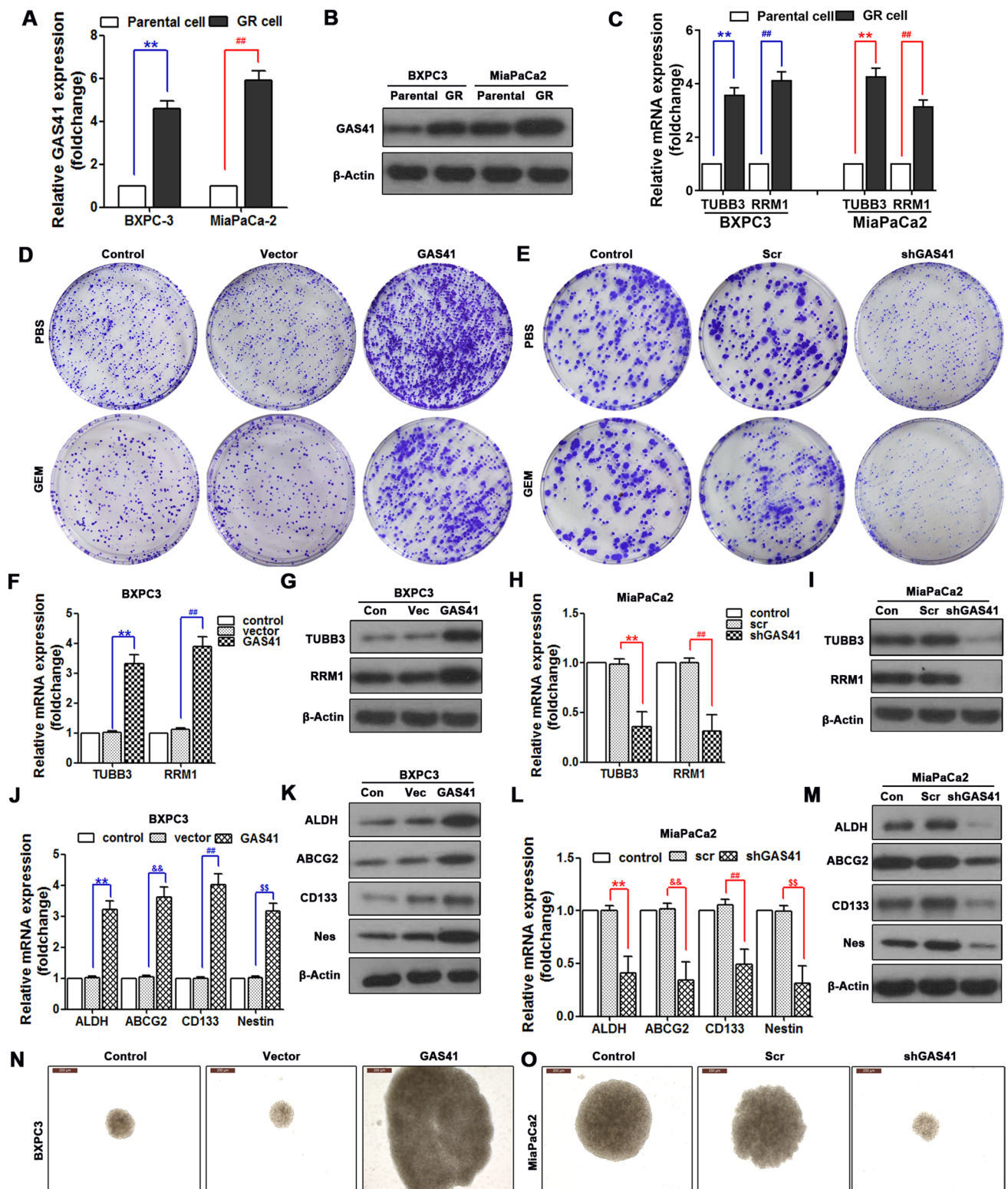
2.1 Human specimens and cell lines

Human pancreatic cancer and adjacent normal tissues were obtained from 87 pancreatic cancer patients who underwent

surgical resection at Shanghai Tenth People's Hospital, Tongji University from 2003 to 2017. Each sample was rapidly cut into two segments of approximately the same size, fixed in formalin and stored in liquid nitrogen. The two segments were later used for histochemical analysis and biomarker testing, respectively. All participating patients provided written informed consent, and the study methodologies conformed to the standards set by the Declaration of Helsinki. All experiments with human tissue samples or animals were approved by the Ethics Committee of Shanghai Tenth People's Hospital. PANC-1, BXPC3, Capan-1, MiaPaCa-2 and SW1990 human pancreatic cancer cell lines and the HPDE human pancreatic duct epithelial cell line were purchased from the ATCC (USA). Cells were maintained in DMEM supplemented with 10% FBS (Sigma, F8318) at 37°C in a humidified atmosphere containing 5% CO₂. The culture medium was changed 3-4 times every week. *GEM* resistance was induced in BXPC-3 and MiaPaCa-2 cells, the two pancreatic cancer cell lines showing the lowest and highest GAS41 expression, respectively, by prolonged *GEM* treatment with stepwise increases in drug concentration. Briefly, BXPC3 and MiaPaCa-2 cells were exposed to 100 nM, 300 nM, 600 nM and 1000 nM *GEM* for 2 weeks at each concentration. *GEM* resistance was confirmed using a MTT assay.

Table 1. GAS41 expression and diagnostic features. (n=87) (Normalized to adjacent cancer tissues)

Characteristics	Low expression (n=31)	High expression (n=56)
	No. of patients (%)	No. of patients (%)
Gender		
Male	18(58.06%)	37(66.07%)
Female	13(41.94%)	19(33.93%)
Age		
21-40	3(9.68%)	8(14.29%)
41-60	11(35.48%)	13(23.21%)
61-80	16(51.61%)	33(58.93%)
81-100	1(3.23%)	2(3.57%)
Histological grade		
Low	8(25.81%)	6(10.71%)
Middle	19(61.29%)	10(17.86%)
High	4(12.90%)	40(71.43%)
TNM stages		
I	4(12.90%)	3(5.35%)
II	16(51.62%)	12(21.43%)
III	11(35.48%)	22(39.29%)
IV	0(0%)	19(33.93%)
Distant metastasis		
No	23(74.19%)	15(26.78%)
Yes	8(25.81%)	41(73.22%)



2.2 Plasmids and transfection

Plasmids expressing GAS41, Notch1, H2A.Z.2, shGAS41, shNotch1, shH2A.Z.2 or scr (scramble shRNA) were generated by GeneChem (Shanghai, China). pLKO.1-shGAS41,

pLKO.1-shNOTCH1 and pLL3.7-shH2A.Z.2 were used for transfection. We used BXPC-3 cells (lowest GAS41 expression) for overexpression and MiaPaCa-2 cells (highest GAS41 expression) for knockdown studies. The transfections were carried out using Lipofectamine 2000 (Invitrogen),

Fig. 2 GAS41 drives pancreatic cancer cell tumorigenesis, stemness and *GEM* resistance. (A, B) *GEM* resistance was induced in BXPC3 and MiaPaCa-2 cells by prolonged *GEM* treatment as described in Materials and Methods. GAS41 mRNA (A) and protein (B) levels in *GEM*-resistant and parental cells determined by qRT-PCR and Western blotting, respectively. (C) mRNA levels of the chemoresistance-related genes TUBB3 and RRM1 analyzed by qRT-PCR. (D-E) Colony formation in the presence or absence of 2 μ M *GEM*. (F-I) mRNA (F, H) and protein (G, I) levels of the chemoresistance-related genes *Tubb3* and *Rrm1* determined by qRT-PCR and Western blotting, respectively. (J-M) mRNA (J, L) and protein (K, M) levels of the stemness-related genes *Aldh*, *Abcg2*, *Cd133* and *Nestin* determined by qRT-PCR and Western blotting, respectively. (N-O) Spheroid formation. $n = 3$, $p < 0.05$, **, ###, &&, \$\$ $p < 0.01$, Scale bars = 200 μ m

11668019) and the transfection efficiencies were assessed using qRT-PCR and Western blotting.

2.3 RNA extraction and qRT-PCR

Total RNA was extracted using TRIzol (Invitrogen, USA). cDNA was synthesized using a PrimeScript RT reagent kit (TaKaRa Bio Inc., Japan). Amplification was performed on an ABI 7900HT real-time PCR system (Applied Biosystems, USA). mRNA levels were calculated using the $2^{-\Delta\Delta Ct}$ method. *Gapdh* was used for internal normalization. The specific primers used in the amplification are listed in the [Supplementary Table](#).

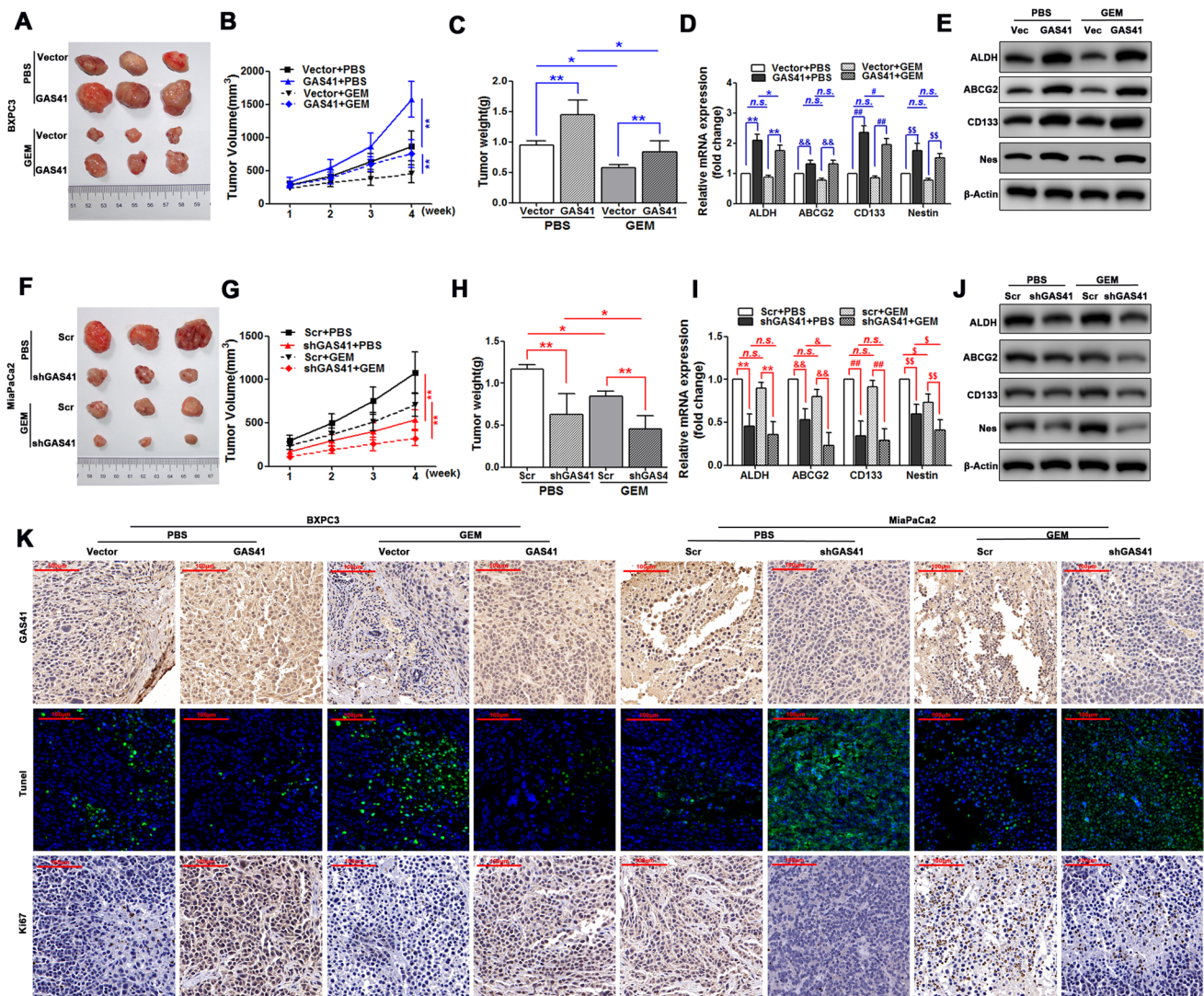
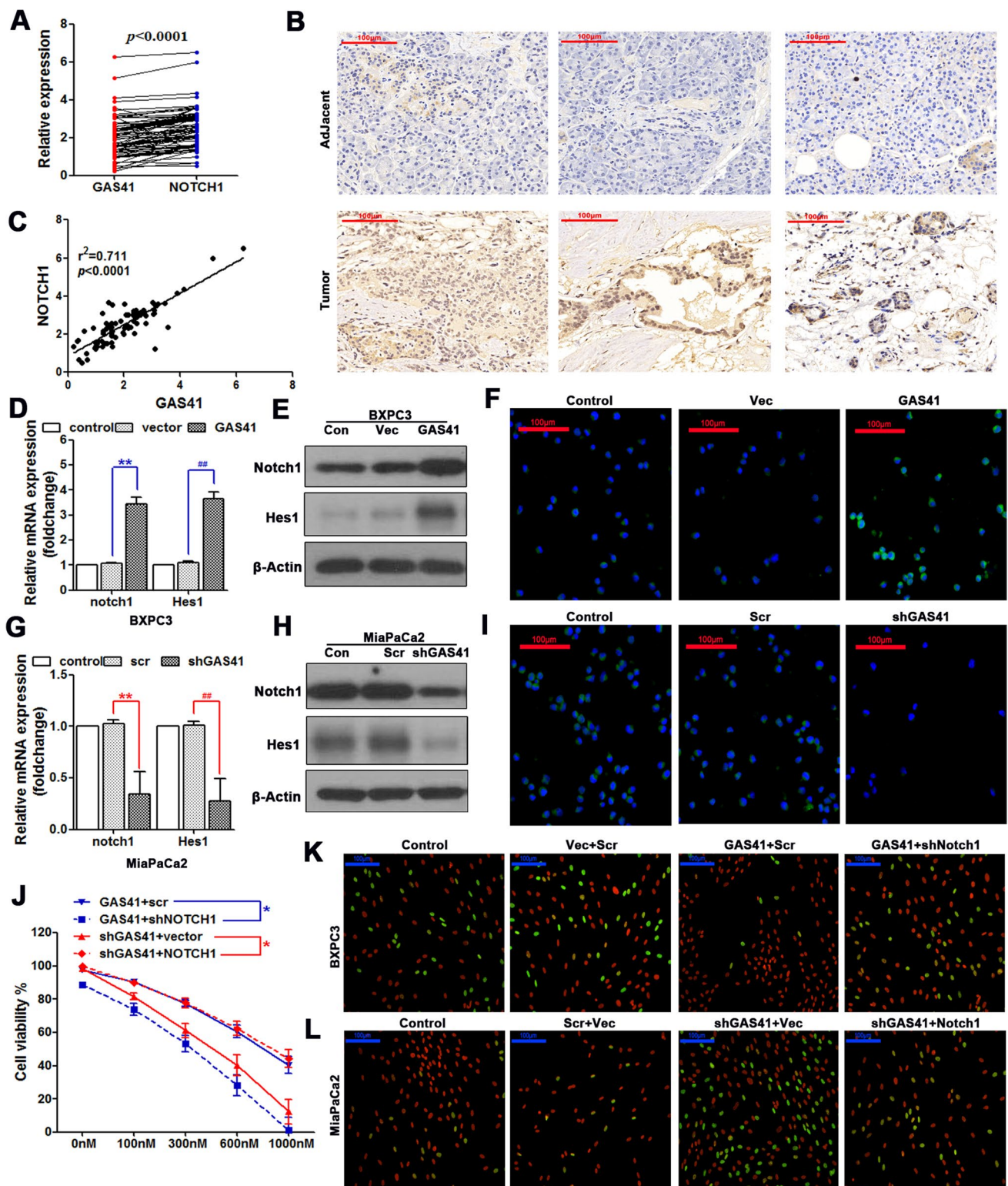


Fig. 3 GAS41 drives pancreatic cancer tumorigenesis and *GEM* resistance *in vivo*. BALB/nu mice were inoculated with BXPC3 cells transfected with vector or GAS41, or with MiaPaCa-2 cells transfected with scr- or shGAS41. The mice were subsequently treated with *GEM* or PBS for 4 weeks as described in Materials and Methods and finally euthanized. (A, F) Photos of the dissected tumors. (B, G) Changes in tumor volume during the 4-week treatment. (C, H)

Weight of the dissected tumors. (D, E, I, J) mRNA (D, I) and protein (E, J) expression of the stemness-related genes *Aldh*, *Abcg2*, *Cd133* and *Nestin* in the tumor samples measured by qRT-PCR and Western blotting, respectively. $n = 5$ mice per group, *, &, #, \$\$ $p < 0.05$, **, &&, ###, \$\$\$ $p < 0.01$, n.s. = no significant difference. (K) IHC staining for GAS41 and Ki67 and TUNEL staining of tumor tissues. Scale bars = 100 μ m



2.4 Chromatin immunoprecipitation (ChIP)

ChIP was carried out as reported previously [23]. Briefly, cells (2×10^7) were incubated with 100 mg/ml recombinant HPA and 1% (v/v) formaldehyde at 37°C for 10 minutes. The

crosslinking reaction was stopped by the addition of glycine, after which the cells were washed with cold PBS. The cells were subsequently lysed in 0.1% NP-40 lysis buffer for 10 minutes on ice. The nuclei were sonicated on ice to break down the nuclear DNA into fragments of one nucleosome (200 bp)

Fig. 4 GAS41 drives tumorigenesis and *GEM* resistance by upregulating NOTCH. (A) mRNA levels of GAS41 and Notch1 in tumor tissues of pancreatic cancer patients (n = 87). (B) IHC staining for NOTCH1 in tumor and adjacent normal tissues of pancreatic cancer patients. (C) Correlation between GAS41 and Notch1 in tumor tissues of pancreatic cancer patients (n = 87). (D-F) BXPC3 cells were transfected with GAS41 or vector for 24 hours. Untransfected cells were included as control. mRNA (D) and protein (E) levels of Notch1 and Hes1 assessed by qRT-PCR and Western blotting, respectively. n = 3, **, ##*p* < 0.01. (F) IHC staining for NOTCH1. Green, NOTCH1; Blue, DAPI; Scale bars = 100 μ m. (G-I) MiaPaCa-2 cells were transfected with shGAS41 or scr for 24 hours. Untransfected cells were included as control. mRNA (G) and protein (H) levels of Notch1 and Hes1 measured by qRT-PCR and Western blotting, respectively. n = 3, **, ##*p* < 0.01. (I) IHC staining for NOTCH1. Green, NOTCH1; Blue, DAPI; Scale bars = 100 μ m. (J-L) BXPC3 cells were co-transfected with GAS41 and scr or GAS41 and shNotch1 for 24 hours. MiaPaCa-2 cells were co-transfected with shGAS41 and vector or shGAS41 and Notch1 for 24 hours. (J) The respective cells were treated with *GEM* at the indicated concentrations for 24 hours. Cell viability was determined by a MTT assay. n = 3, **p* < 0.05. (K, L) IF TUNEL staining. Green, fragmented DNA; Red, nucleus Scale bars = 100 μ m

in length. The resulting chromatin solution (500 μ g) was incubated overnight at 4°C with ChIP-grade anti-GAS41 (Abcam, ab251981) and anti-rabbit IgG (Abcam, ab172730) antibodies. The H2A.Z.2-DNA complexes were precipitated and the DNA fragments were purified using a QIAquick PCR purification kit (Qiagen, USA). The purified samples were analyzed by PCR using primers specific for the human *Notch1* and *Hes1* promoters. The pre-ChIP DNA samples were used as the input control in each PCR. The ChIP-PCR primers used in the amplification are listed in the [Supplementary Table](#).

2.5 Western blot analysis and co-immunoprecipitation (co-IP)

Cells were lysed in cold lysis buffer (50 mM Tris-HCl, pH 7.4, 250 mM NaCl, 0.5% Triton X-100, 10% glycerol, 1 mM DTT) containing protease inhibitors. The proteins were separated by 10-12% SDS-PAGE and transferred to nitrocellulose membranes. After blocking in Pierce™ Protein-Free Blocking Buffer (Thermo Scientific™, 37570), the membranes were incubated overnight at 4°C with antibodies directed against GAS41 (Abcam, ab251981), ALDH (Invitrogen, PA5-27414), ABCG2 (Abcam, ab207732), CD133 (Abcam, ab216323), NESTIN (Abcam, ab105389), TUBB3 (Abcam, ab52623), RRM1 (Abcam, ab137114), NOTCH1 (Sigma, SAB5200906), HES1 (Abcam, ab108937) and H2AZ (Abcam, ab4174). After incubation with the corresponding secondary antibodies, immunoreactivity was detected using an enhanced chemiluminescence (ECL) system (Millipore, USA). Co-IP experiments were performed as described previously [24]. Briefly, MiaPaCa-2 cells transfected with H2A-eGFP- or H2A.Z.2-eGFP-expressing plasmids were lysed in cold

lysis buffer containing protease inhibitors. pcDNA3.1/c-eGFP, pcDNA3.1/GAS41-c-eGFP or pcDNA3.1/H2A.Z.2-c-eGFP were used in co-IP experiments. To this end, the lysates were incubated with non-specific antibody-coated protein A/G beads (Millipore) or anti-eGFP-conjugated agarose beads (Sigma) overnight at 4°C. After washing in cell lysis buffer, the bound proteins were eluted with SDS buffer and analyzed by Western blotting.

2.6 Immunohistochemistry (IHC), immunofluorescence (IF) and TUNEL assays

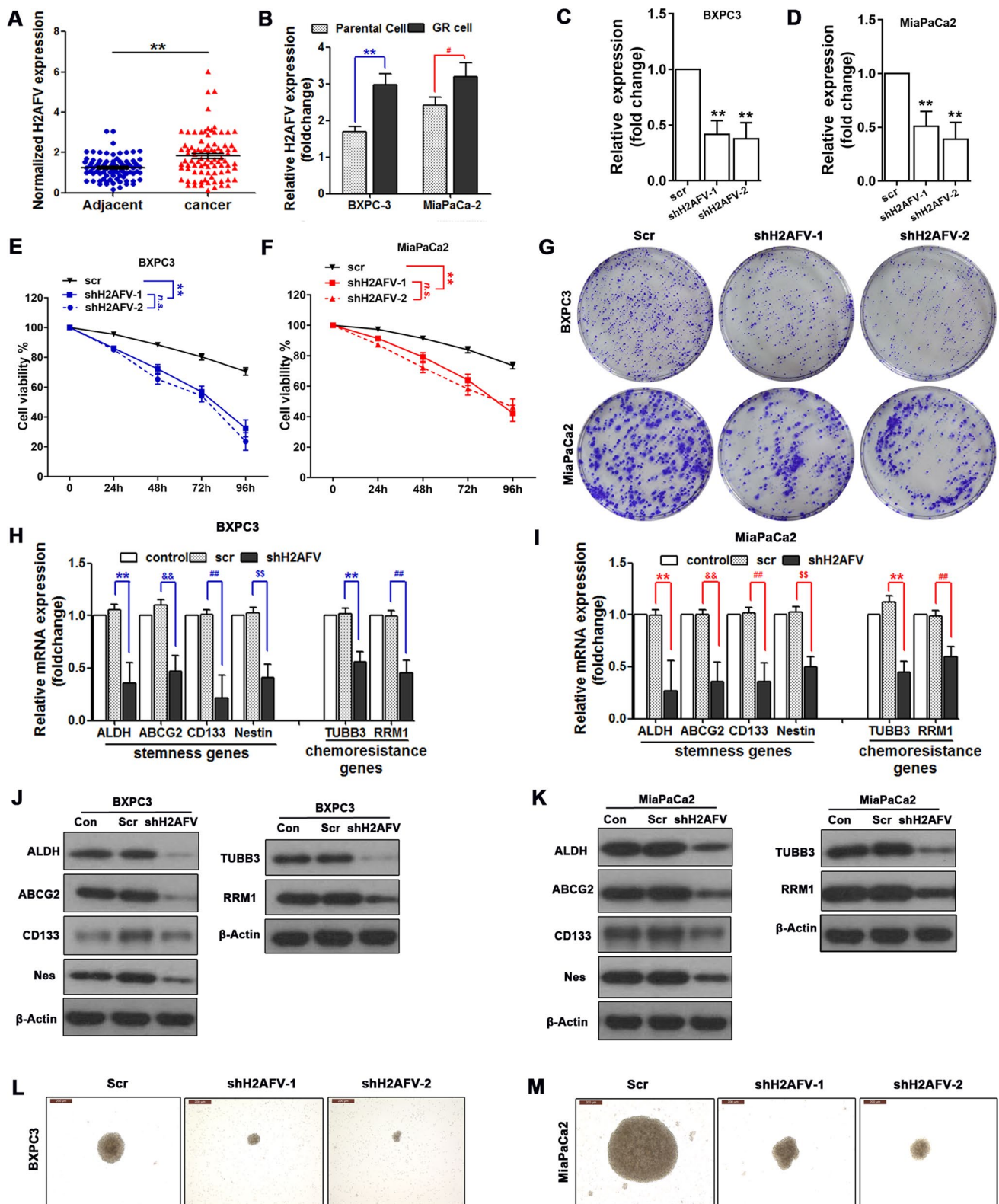
In situ IHC staining for GAS41 (Abcam, ab251981), NOTCH1 (Sigma, SAB5200906), and Ki-67 (Abcam, ab15580) was performed using the corresponding IHC kits. *In situ* cell apoptosis was detected using TUNEL assay kit - HRP-DAB (Abcam, ab206386). To detect NOTCH1 by IF, cells were incubated with anti-NOTCH1 antibody (1:200; SAB5200906) in PBS containing 1% BSA at 37°C for 1 hour followed by incubation with goat anti-rabbit IgG H&L (Alexa Fluor® 488) (Abcam, ab150077) at room temperature for 1 hour. Nuclei were visualized with DAPI (Sigma, D9542). Images were acquired on an inverted fluorescence microscope (Nikon, Japan).

2.7 Cell proliferation and colony formation assays

To evaluate proliferation, cells were seeded in 96-well plates (2-4 × 10³ cells per well). After 24-hour incubation, the cells were treated with different concentrations of *GEM* at 37°C for 0-96 hours. Cell viability was determined using a CyQUANT™ MTT Cell Viability Assay Kit (Invitrogen, V13154) and the absorbance at 490 nm was recorded on a microplate reader. The half-maximal inhibitory concentration (IC₅₀) of *GEM* was determined using Sigma Plot 9.0 software (Systat Software Inc., USA). To evaluate colony formation, cells were seeded in 6-well plates (500-600 cells per well). After 24-hour incubation, the cells were treated with 2 μ M *GEM* or PBS at 37°C for 24 hours. Next, the cells were incubated in drug-free growth medium for another 14 days, fixed with 4% formaldehyde, and stained with 0.5% crystal violet. The numbers of colonies were counted in 5 fields. Each experiment was repeated three times.

2.8 Spheroid formation assay

Cells were seeded into 24-well Corning® Costar® ultra-low adhesion plates (Sigma, CLS3473) (1 × 10⁴ per well) and cultured in cancer stem cell medium (McCoy's 5A



medium supplemented with 10 ng/ml EGF, 20 ng/ml bFGF, 5 μ g/ml insulin, 0.4% BSA, and 2% B27) for 10 days. The formation of spheroids was evaluated under a microscope.

2.9 *In vivo* tumorigenesis assay

BALB/nu mice (6-8 weeks old) were obtained from the Shanghai Lab Animal Research Center (Shanghai,

Fig. 5 H2A.Z.2 mediates pancreatic cancer cell tumorigenesis, stemness and *GEM* resistance. (A) H2A.Z.2 mRNA levels in human pancreatic cancer and adjacent normal tissues determined by qRT-PCR. $n = 87$, $**p < 0.01$. (B) H2A.Z.2 mRNA levels in wild-type and GR BXPC3 and MiaPaCa-2 cells assessed by qRT-PCR. $n = 3$, $^{\#}p < 0.05$, $**p < 0.01$. (C, E, G-upper panel) BXPC3 cells were transfected with shH2A.Z.2-1, shH2A.Z.2-2 or scr for 24 hours. (C) H2A.Z.2 mRNA levels examined by qRT-PCR. (E) Cell viability assessed after treatment with the indicated concentrations of *GEM* for 24-96 hours using a MTT assay. (G-upper panel) Colony formation. $n = 3$, $**p < 0.01$, *n.s.* = no significant difference. (D, F, G-lower panel) MiaPaCa-2 cells were transfected with shH2A.Z.2-1, shH2A.Z.2-2 or scr for 24 hours. (D) H2A.Z.2 mRNA levels examined by qRT-PCR. (F) Cell viability assessed after treatment with the indicated concentrations of *GEM* after 24-96 hours treatment using a MTT assay. (G-lower panel) Colony formation. $n = 3$, $**p < 0.01$, *n.s.* = no significant difference. (H, J) BXPC3 cells were transfected with shH2A.Z.2 or scr for 24 hours. Untransfected cells were included as control. mRNA (H) and protein (J) expression of the stemness- and chemoresistance-related genes determined by qRT-PCR and Western blotting, respectively. $n = 3$, $**$, $\&\&$, $\#\#$, $\$\$$ $p < 0.01$. (I, K) MiaPaCa-2 cells were transfected with shH2A.Z.2 or scr for 24 hours. Untransfected cells were included as control. mRNA (I) and protein (K) levels of stemness- and chemoresistance-related genes determined by qRT-PCR and Western blotting, respectively. $n = 3$, $**$, $\&\&$, $\#\#$, $\$\$$ $p < 0.01$. (L, M) Spheroid formation of BXPC3 (L) and MiaPaCa-2 (M) cells transfected with sh-1H2A.Z.2, sh-2H2A.Z.2 or scr

China). 2×10^6 cells in 100 μ l PBS were subcutaneously injected into the left flank of each mouse. When palpable tumors were formed, the animals were divided into two groups and administered intraperitoneal *GEM* (20 mg/kg) or PBS (100 μ l) twice a week for four weeks. The tumor lengths and widths were measured twice a week using an external caliper. The tumor volumes were calculated using the equation $V = (\text{length} \times \text{width}^2)/2$. The mice were sacrificed at the end of the experiments after which the tumors were harvested for examination. The study methodologies used were in conformity with the standards set by the Declaration of Helsinki and were approved by the Ethics Committee of the Shanghai Tenth People's Hospital.

2.10 Statistical analysis

Data are presented as the means \pm SD (standard deviation). Comparisons between groups were carried out using one-way ANOVA and Tukey's test. Associations between GAS41 and Notch1 expression were analyzed using Pearson correlation analysis. Survival analysis was performed using the Kaplan-Meier method. The average expression of GAS41 was used during survival analysis. SPSS 13.0 software (IBM, USA) was used for statistical interpretations. *P*-values < 0.05 were considered to be statistically significant.

3 Results

3.1 GAS41 is overexpressed in human pancreatic cancer tissues and cell lines

To assess the role of GAS41 in pancreatic cancer, we first examined its expression in human pancreatic cancer tissues and cell lines. Using qRT-PCR, we found that, compared with adjacent normal tissues, human pancreatic cancer tissues exhibited significantly higher GAS41 mRNA expression levels (Fig. 1A). An association between GAS41 expression levels and patient characteristics is shown in Table 1. The cancerous tissues also exhibited higher GAS41 protein expression levels as revealed by Western blotting and IHC (Fig. 1B, C). In addition, using Kaplan-Meier survival analysis, we observed a positive association between high tumorous GAS41 expression and a poor survival (Fig. 1D). Consistent with these clinical data, four out of the five human pancreatic cancer cell lines tested in this study showed significantly higher GAS41 expression levels than the HPDE pancreatic epithelial cell line (Fig. 1E, F). Of note, we found that the proliferation of the five cancerous cell lines in the presence of 2 μ M *GEM* correlated with their GAS41 expression levels (Fig. 1G), implicating a role of GAS41 in drug resistance. Thus, our data indicate that GAS41 is overexpressed in human pancreatic cancer tissues and cell lines.

3.2 GAS41 drives pancreatic cancer cell development, stemness and *GEM* resistance

To assess the role of GAS41 in *GEM* resistance, we chose to study BXPC-3 and MiaPaCa-2, the two pancreatic cancer cell lines showing the lowest and highest GAS41 expression levels, respectively (Fig. 1E, F). After prolonged *GEM* treatment with a stepwise increase in drug concentration, these cells developed *GEM* resistance (GR) as manifested by an approximately 3.5-4-fold increase in the IC_{50} value of *GEM* (Sup Fig. 1A, B). Of note, GAS41 expression was increased in the GR cells (Fig. 2A, B). In addition, we found that the GR cells exhibited increased expression levels of the chemoresistance-related genes *Tubb3* and *Rrm1* (Fig. 2C), as well as the stemness-related genes *Aldh*, *Abcg2*, *Cd133* and *Nestin* (Sup Fig. 1C-D) compared to the corresponding wild-type cells. We subsequently transfected BXPC-3 cells with GAS41-expressing plasmids and MiaPaCa-2 cells with shGAS41-expressing plasmids. GAS41 overexpression and knockdown were subsequently confirmed using qRT-PCR and Western blotting (Sup Fig. 1E-F). We found that GAS41 overexpression in BXPC-3 cells promoted their proliferation (Sup Fig. 1G), colony forming (Fig. 2D, upper panel) and spheroid forming (Fig. 2N) capacities, and

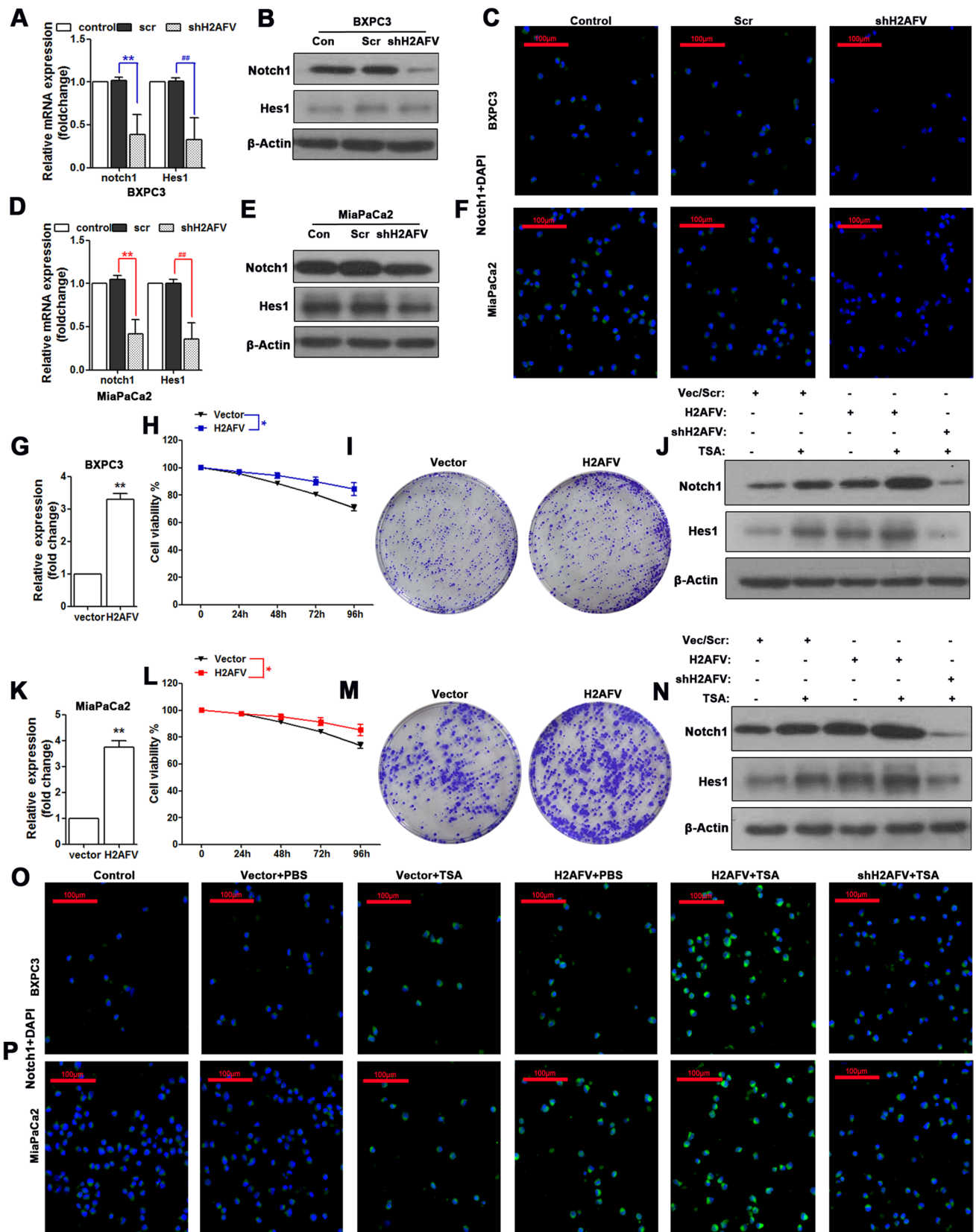


Fig. 6 **AcH2A.Z.2 upregulates Notch.** (A-F) BXPC3 (A-C) and MiaPaCa-2 (D-F) cells were transfected with shH2A.Z.2 or scr for 24 hours. Untransfected cells were included as control. (A, D) mRNA levels of *Notch1* and *Hes1* levels assessed by qRT-PCR. $n = 3$, $^{**}p < 0.01$. (B, E) Protein levels of NOTCH1 and HES1 examined by Western blotting. (C, F) IF staining for NOTCH1. Green, NOTCH1; Blue, DAPI; Scale bars = 100 μm . (G-I, K-M) BXPC-3 (G-I) and MiaPaCa-2 (K-M) cells were transfected with H2A.Z.2 or vector for 24 hours. (G, K) mRNA levels of H2A.Z.2 assessed by qRT-PCR. (H, L) Cell viability assessed after treatment with the indicated concentrations of *GEM* for 24-96 hour by a MTT assay. (I, M) Colony formation. $n = 3$, $^{*}p < 0.05$, $^{**}p < 0.01$. (J, N, O, P) BXPC3 (J, O) and MiaPaCa-2 (N, P) cells were transfected with H2A.Z.2, vector, shH2A.Z.2 or scr for 24 hours with or without pretreatment with TSA (200 nM) for 2 hours as indicated. (J, N) NOTCH1 and HES1 protein levels were examined by Western blotting. (O, P) IF staining for NOTCH1. Green, NOTCH1; Blue, DAPI; Scale bars = 100 μm

induced resistance to *GEM* (Fig. 2D, lower panel). GAS41 knockdown in MiaPaCa-2 cells inhibited their proliferation (Sup Fig 1G), colony forming (Fig. 2E, upper panel) and spheroid forming (Fig. 2O) capacities, and sensitized the cells to *GEM* (Fig. 2E, lower panel). These data support a role of GAS41 as driver of tumorigenesis and drug resistance. Mechanistically, we found that GAS41 overexpression increased the expression of chemoresistance- (Fig. 2F, G) and stemness-related genes (Fig. 2J-K), while GAS41 knockdown had the opposite effect (Fig. 2H, I and L, M). We subsequently examined the effects of GAS41 overexpression and knockdown in the corresponding GR cells and obtained similar results (Sup Fig. 1H-L). These data suggest that GAS41 drives tumorigenesis, stemness and *GEM* resistance in pancreatic cells *in vitro*.

3.3 GAS41 drives pancreatic cancer tumorigenesis and *GEM* resistance *in vivo*

To determine whether our *in vitro* findings can be extrapolated *in vivo*, we established xenograft mouse models of human pancreatic cancer using genetically modified BXPC3 and MiaPaCa-2 cells. We found that compared with control tumors, tumors derived from GAS41-overexpressing BXPC3 cells exhibited a faster growth rate and greater *GEM* tolerance (Fig. 3A-C), along with higher expression levels of the stemness-related markers *Aldh*, *Abcg2*, *Cd133* and *Nes* (Fig. 3D, E). In contrast, we found that tumors derived from GAS41-silenced MiaPaCa-2 cells were smaller and exhibited a decreased *GEM* tolerance (Fig. 3F-H), as well as lower expression levels of the stemness-related markers (Fig. 3I-J). Consistent with these findings, GAS41-overexpressing tumors exhibited higher levels of Ki67 expression (a proliferation marker) and lower apoptotic rates as indicated by IHC and TUNEL staining (Fig. 3K), while GAS41-silenced tumors showed decreased Ki67 expression levels and increased apoptotic rates (Fig. 3K). Thus, similar to our

in vitro findings, we found that GAS41 promotes pancreatic cancer cell stemness and drives tumorigenesis and *GEM* resistance *in vivo*.

3.4 GAS41 drives tumorigenesis and *GEM* resistance by upregulating Notch

The NOTCH pathway has been shown to mediate the stem-like transition of GR pancreatic cancer cells [12]. To explore whether NOTCH can mediate the pro-stemness and pro-resistance activities of GAS41, we examined *Notch* expression in pancreatic cancer tissue samples using qRT-PCR and IHC. Higher NOTCH levels were detected in tumor tissues compared to adjacent normal tissues (Fig. 4B). Of note, Notch expression positively correlated with GAS41 expression in the tumor tissues (Fig. 4A, C), suggesting a regulatory relationship. *Hes1*, a downstream mediator of *Notch*, is known to play a key role in stemness and chemoresistance in various cancers [25]. Here, we found that GAS41 overexpression increased the mRNA and protein expression levels of Notch1 and Hes1 in wild-type (Fig. 4D-F) and GR BXPC-3 cells (Fig. 4D-F, Sup Fig. 2A, B), while GAS41 knockdown in wild-type (Fig. 4G-I) and GR MiaPaCa-2 cells (Sup Fig. 2C, D) had the opposite effect. To further explore the relationship between GAS41 and Notch, we co-transfected wild-type or GR BXPC-3 cells with GAS41- and shNotch1-expression plasmids, and wild-type or GR MiaPaCa-2 cells with shGAS41- and Notch1-overexpression plasmids. Notch1 overexpression and knockdown were confirmed by qRT-PCR and Western blotting (Sup Fig. 2E-H). We found that Notch1 knockdown reduced the *GEM* tolerance increased by GAS41 overexpression, and that Notch overexpression increased the *GEM* tolerance reduced by GAS41 knockdown (Fig. 4J, Sup Fig. 2I). Moreover, we found after IF TUNEL staining that Notch1 knockdown in wild-type BXPC-3 cells restored the apoptosis inhibited by GAS41 overexpression (Fig. 4K), while Notch1 overexpression in wild-type MiaPaCa-2 cells reduced the apoptosis induced by GAS41 knockdown (Fig. 4L). Collectively, these results indicate that GAS41 drives tumorigenesis and *GEM* resistance by upregulating Notch1.

3.5 H2A.Z.2 mediates pancreatic cancer cell tumorigenesis, stemness and *GEM* resistance

Given the reported function of H2A.Z.2 in malignancy and chemoresistance [17], we speculated that H2A.Z.2 might be involved in pancreatic cancer tumorigenesis and drug resistance. Indeed, we found that H2A.Z.2 was overexpressed in human pancreatic cancer tissues (Fig. 5A), and that its expression in pancreatic cancer cells correlated with *GEM* resistance (Fig. 5B). In addition, we analyzed

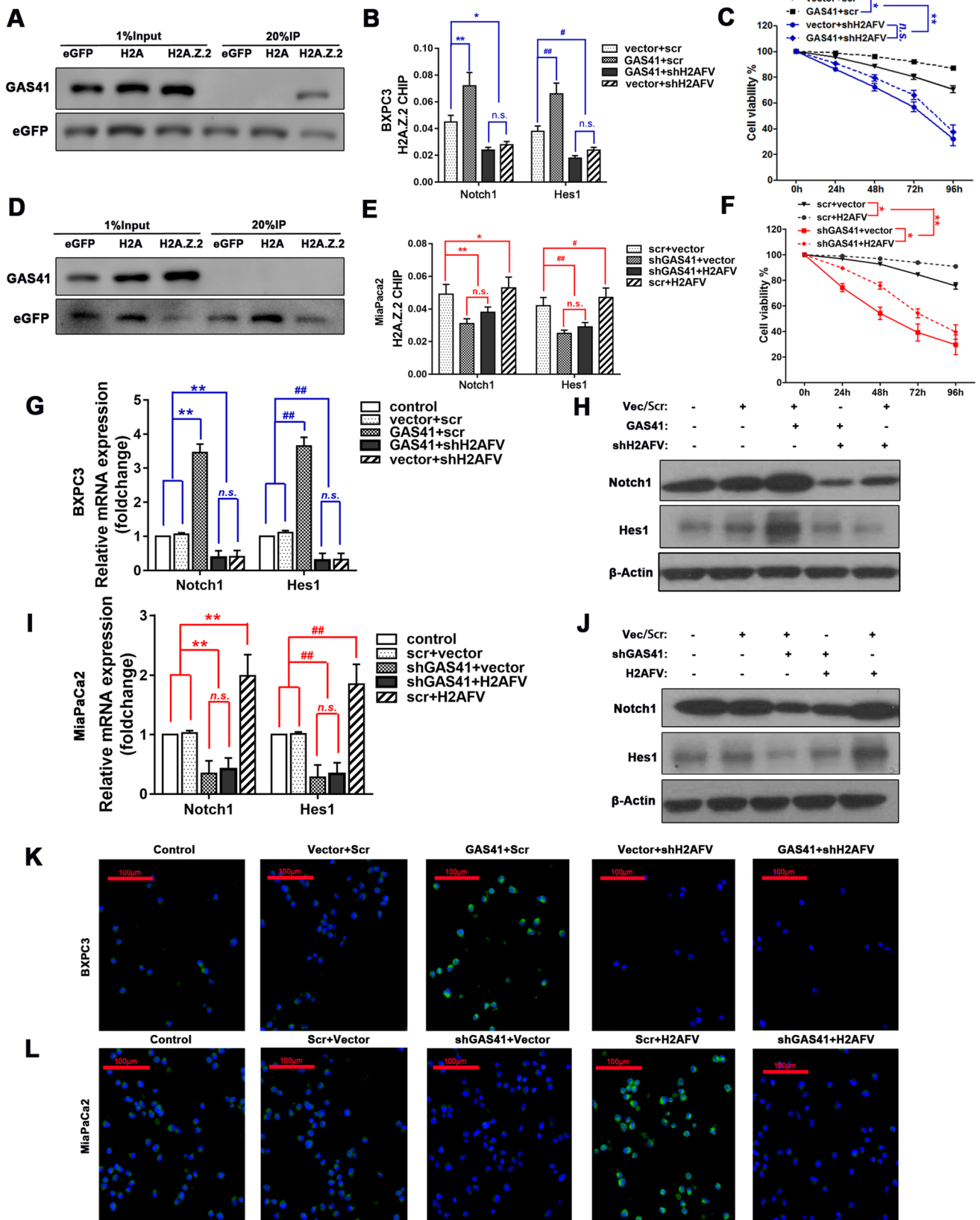


Fig. 7 GAS41 activates *Notch* and its downstream mediators. (A, D) MiaPaCa-2 cells transfected with eGFP-, H2A-eGFP- or H2A.Z.2-eGFP-expressing plasmids were subjected to co-IP as described in Materials and Methods in the absence (A) or presence (D) of a deacetylase. (B, C, E, F, G-L) BXPC3 cells (B, C, G, H, K) were transfected with GAS41, shH2A.Z.2, vector or scr, either alone or in combination as indicated. MiaPaCa-2 cells (E, F, I, J, L) were transfected with shGAS41, H2A.Z.2, vector or scr, either alone or in combination as indicated. (B, E) ChIP analysis performed with primers targeted to the promoter regions of Notch1 and Hes1. (C, F) Cell viability assessed after treatment with the indicated concentrations of *GEM* for 24-96 hour using a MTT assay. (G-J) The mRNA (G, I) and protein (H, J) levels of Notch and Hes1 examined by qRT-PCR and Western blotting, respectively. (K, L) IF staining for NOTCH1. Green, NOTCH1; Blue, DAPI; Scale bars = 100 μ m. n = 3, *[#]*p* < 0.05, **[#]*p* < 0.01, n.s. = no significant difference

H2A.Z.2.1 and H2A.Z.1 expression by qRT-PCR in tissue samples, and found that both were overexpressed in pancreatic cancer tissues. (Sup Fig. 3A, B) We subsequently transfected BXPC3 and MiaPaCa-2 cells with shH2A.Z.2- or H2A.Z.2-expressing plasmids, respectively. H2A.Z.2 knockdown (Sup Fig. 3C-D) and overexpression (Sup Fig. 3E-F) were confirmed by qRT-PCR and Western blotting (Fig. 5C, D; Fig. 6G, K). Since a higher interference efficiency was observed for shH2AFV-2 than shH2AFV-1, we used shH2AFV-2 for subsequent experiments. We also found that H2A.Z.2 expression increased in pancreatic cancer cells (Sup Fig. 3G). Similar to GAS41 knockdown, we found that H2A.Z.2 knockdown inhibited the proliferation, colony forming and spheroid forming capacities (Fig. 5E-G, L, M) and reduced the expression of stemness- and chemoresistance-related genes (Fig. 5H-K) in these cells. H2A.Z.2 knockdown restored their sensitivity to *GEM* (Sup Fig. 4B, D), as well as reduced the expression of stemness and chemoresistance markers in GR cells (Sup Fig. 4E-J). In contrast, we found that H2A.Z.2 overexpression promoted colony formation and increased *GEM* tolerance (Fig. 6H, I, L, M). These data directly link H2A.Z.2 to pancreatic cancer cell tumorigenesis, stemness and chemoresistance.

3.6 Acetylated H2A.Z.2 (acH2A.Z.2) upregulates Notch

Chromatin deposition of acetylated H2A.Z has been linked to the activation of Notch [15]. Here, we found that H2A.Z.2 knockdown in BXPC3 and MiaPaCa-2 cells led to decreased Notch1 and Hes1 mRNA and protein expression levels (Fig. 6A-F), while its overexpression had the opposite effect (Fig. 6J, N, O, P), indicating that H2A.Z.2 upregulates Notch. This regulatory relationship was also observed in GR cells (Sup Fig. 5A-D). To determine whether this activity of H2A.Z.2 depends on its acetylation, we examined the effects of trichostatin A (TSA), a selective histone deacetylase (HDAC) inhibitor. Similar to H2A.Z.2 overexpression,

we found that TSA treatment alone also increased NOTCH1 and HES1 protein expression levels (Fig. 6J, N, O, P), suggesting that acH2A.Z.2 mediates the activation of NOTCH. This notion was further supported by the subsequent finding that TSA augmented NOTCH and HES1 expression increased by H2A.Z.2 overexpression, and partially restored NOTCH1 and HES1 protein expression reduced by H2A.Z.2 knockdown (Fig. 6J, N, O, P). These findings suggest that acH2A.Z.2 upregulates Notch.

3.7 GAS41 activates *Notch* and its downstream mediators

A recent study has shown that GAS41 can bind to acetylated histone H3 to promote H2A.Z deposition onto chromatin in non-small cell lung cancer (NSCLC) [20]. Given this function of GAS41 as a reader of histone acetylation, we speculated that GAS41 may bind to acH2A.Z.2. In line with this hypothesis, we observed using co-IP a direct interaction between GAS41 and H2A.Z.2 in MiaPaCa-2 cells (Fig. 7A). However, this interaction was lost after the addition of C646, a histone acetylase inhibitor (Fig. 7D), indicating that GAS41 binds to acH2A.Z.2, but not its deacetylated counterpart. We subsequently performed ChIP experiments to evaluate the deposition of H2A.Z.2 onto the promoter regions of Notch1 and Hes1. As speculated, we found that GAS41 overexpression in BXPC3 cells increased H2A.Z.2 binding to the Notch1 and Hes1 promoters, while GAS41 knockdown in MiaPaCa-2 cells decreased H2A.Z.2 binding to the Notch1 and Hes1 promoters. (Fig. 7B, E; Sup Fig. 5E-F). Of note, we found that H2A.Z.2 overexpression in GAS41 knockdown MiaPaCa-2 cells failed to restore H2A.Z.2 binding to the Notch1 and Hes1 promoters (Fig. 7E), indicating that GAS41 is indispensable for the deposition of H2A.Z.2 at the Notch1 and Hes1 promoters. In addition, we found that the Notch1 and Hes1 mRNA and protein levels were dependent on GAS41 expression (Fig. 7G-L), confirming that GAS41 can activate *Notch* and its downstream mediators.

3.8 GAS41 in combination with H2A.Z.2 drives pancreatic cancer cell tumorigenesis, stemness and *GEM* resistance

Based on the observed GAS41/H2A.Z.2/Notch regulation in pancreatic cancer cells, we next set out to examine its role in tumorigenesis, stemness and *GEM* resistance. Expression of stemness- and chemoresistance-related genes was detected in BXPC3 and MiaPaCa-2 cells with knockdown or overexpression of GAS41 and H2AFV (Fig. 8A-H). The combination of GAS41 and H2A.Z.2 positively regulated gastric cancer cell tumorigenesis and stemness. Increased stemness was also observed in the spheroid formation assay (Fig. 8I, J,

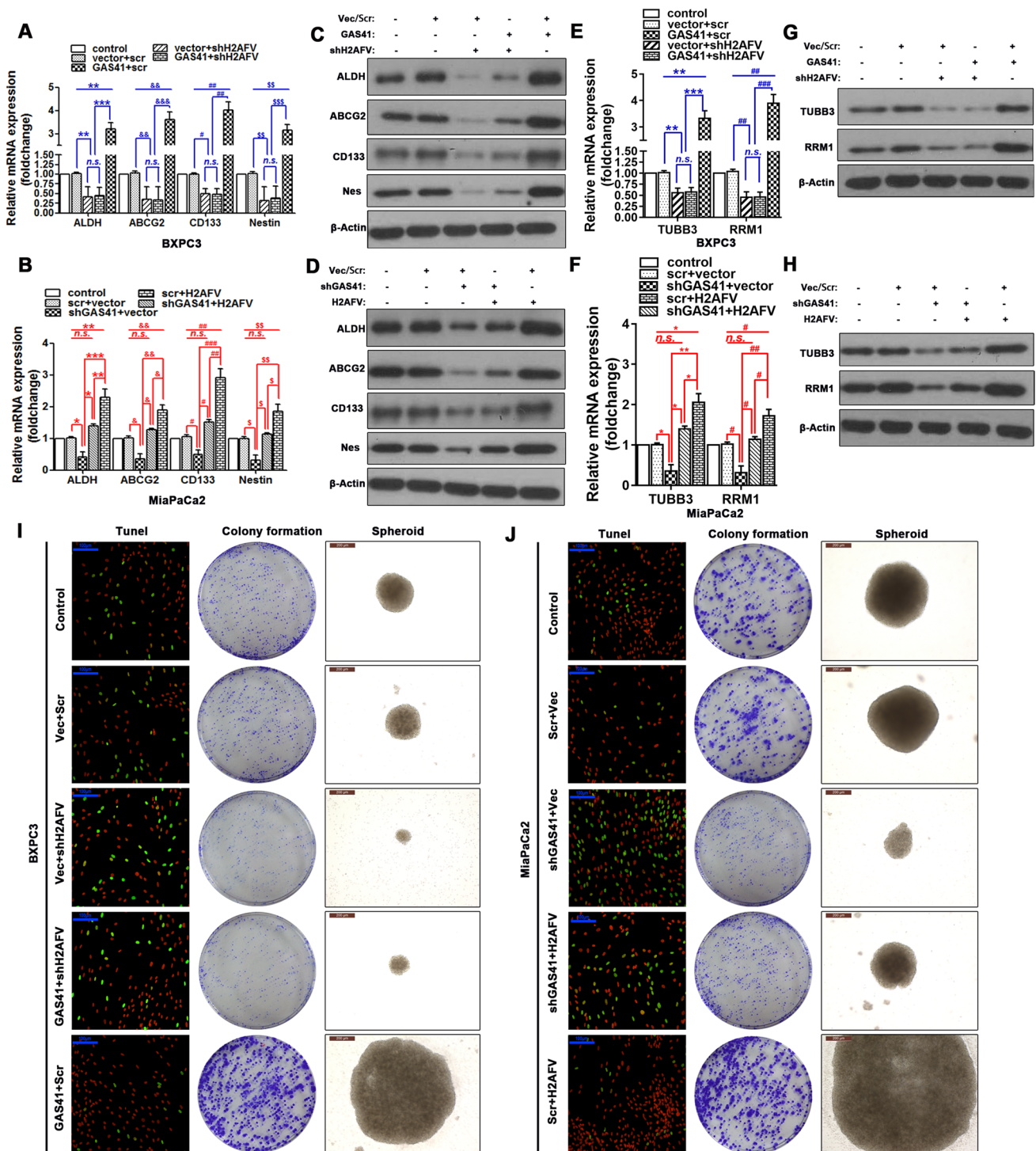


Fig. 8 GAS41 in combination with H2A.Z.2 drives pancreatic cancer cell tumorigenesis, stemness and *GEM* resistance. BXPC3 cells (A, C, E, G, I) were transfected with GAS41, shH2A.Z.2, vector or scr, either alone or in combination as indicated. MiaPaCa-2 cells (B, D, F, H, J) were transfected with shGAS41, H2A.Z.2, vector or scr, either alone or in combination as indicated. Untransfected cells were included as controls. (A-H) mRNA (A, B, E, F) and protein (C,

D, G, H) levels of the stemness- and chemoresistance-related genes assessed by qRT-PCR and Western blotting, respectively. $n = 3$, *, #, &, S $p < 0.05$, **, ##, &&, \$\$\$ $p < 0.01$, ***, ###, &&&, \$\$\$S $p < 0.001$, n.s. = no significant difference. (I-left, J-left) IF TUNEL staining. Scale bars = 100 μ m. (I-center, J-center) Colony formation after 24-hour treatment with 2 μ M *GEM*. Scale bars = 100 μ m. (I-right, J-right) Spheroid formation. Scale bars = 200 μ m

right panels). Similarly, we found that colony formation was increased (Fig. 8I, J, center panels) and apoptosis was decreased (Fig. 8I, J, left panels) when the cells were treated with *GEM*. Thus, GAS41 in combination with H2A.Z.2 drives pancreatic cancer cell tumorigenesis, stemness and *GEM* resistance through Notch.

3.9 GAS41 in combination with H2A.Z.2 drives pancreatic cancer tumorigenesis, stemness and *GEM* resistance *in vivo*

To investigate the function of GAS41 in combination with H2A.Z.2 in pancreatic cancer *in vivo*, we studied xenograft

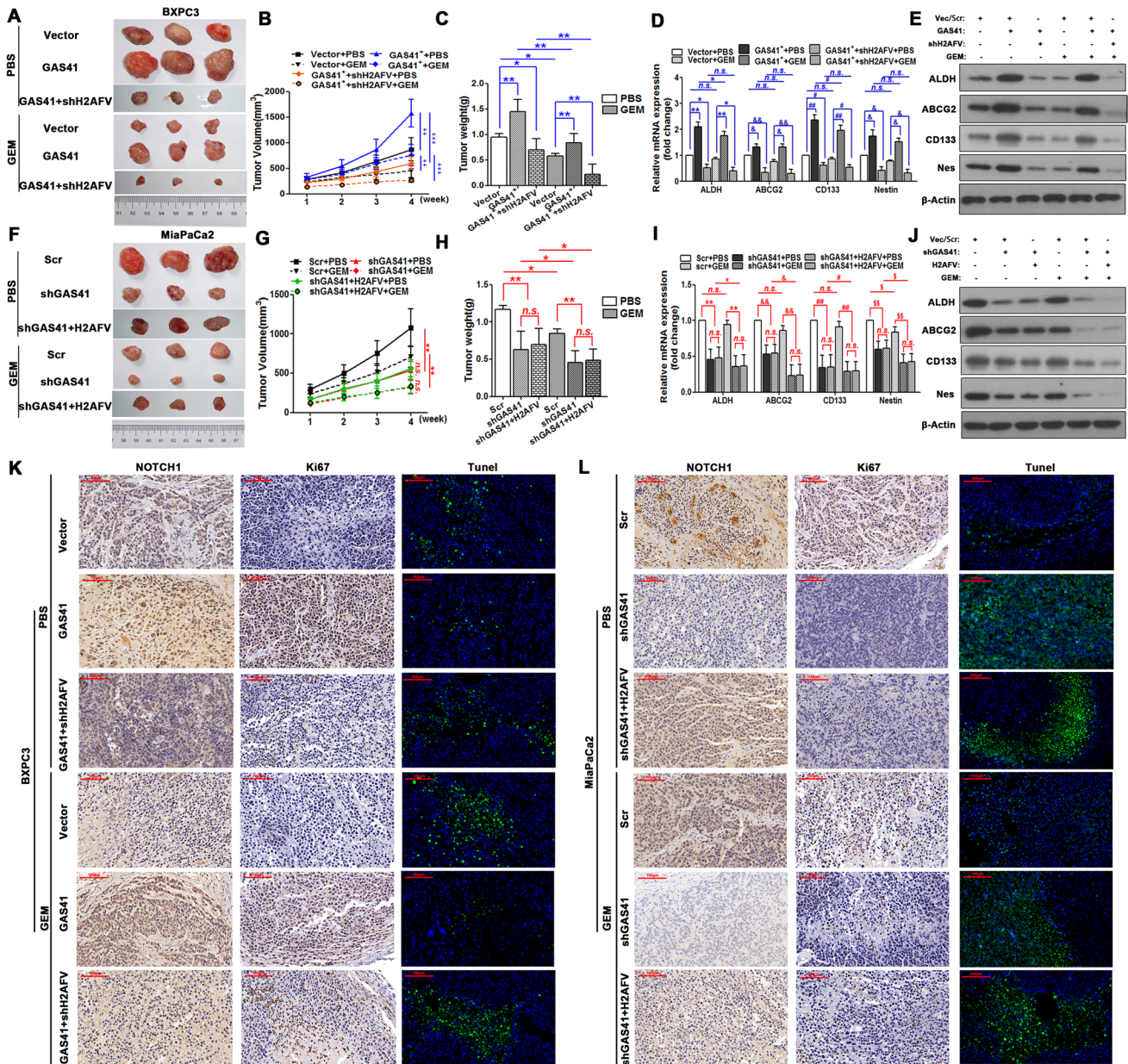


Fig. 9 GAS41 in combination with H2A.Z.2 drives pancreatic cancer tumorigenesis, stemness and *GEM* resistance *in vivo*. BALB/nu mice were inoculated with BXPC3 cells transfected with vector, GAS41 or GAS41+shH2A.Z.2 (A-E, K) or with MiaPaCa-2 cells transfected with scr-, shGAS41 or shGAS41+H2A.Z.2 (F-J, L). The mice were subsequently treated with PBS or *GEM* for 4 weeks as described in Materials and Methods, and finally euthanized. (A, F) Photographs of the dissected tumors. (B, G) Changes in tumor

volume during the 4-week treatment. (C, H) Weight of the dissected tumors. (D-J) mRNA (D, I) and protein (E, J) levels of the stemness-related genes *Aldh*, *Abcg2*, *Cd133* and *Nestin* in tumor tissues examined by qRT-PCR and Western blotting, respectively. (K, L) IHC staining for NOTCH1 and Ki67 and TUNEL staining of tumor tissues. Scale bars = 100 μm. n = 5 mice per group. *, &, #, \$ *p* < 0.05, **, &&, ##, \$\$ *p* < 0.01, *** *p* < 0.001, n.s. = no significant difference

tumors derived from BXPC3 cells transfected with vector, GAS41 or GAS41+shH2A.Z.2, and from MiaPaCa-2 cells transfected with scr-, shGAS41 or shGAS41+H2A.Z.2. We found that GAS41-overexpressing tumors exhibited a more rapid growth and a greater *GEM* resistance and stemness than GAS41-silenced tumors. However, H2A.Z.2 knockdown decreased the tumorigenesis, stemness and *GEM* resistance induced by GAS41 overexpression (Fig. 9A-E,K), while H2A.Z.2 overexpression failed to restore the tumorigenesis, stemness and resistance reduced by GAS41 knockdown (Fig. 9F-J,L). These results indicate that both GAS41 and H2A.Z.2 are required to upregulate Notch-mediated tumorigenesis, stemness and *GEM* resistance of pancreatic cancer cells *in vivo*.

4 Discussion

Histone acetylation and deacetylation are fundamental processes involved in epigenetic regulation of gene expression. Abnormal patterns of histone acetylation are closely associated with human cancer and thus, understanding the mechanisms of histone acetylation reading and writing are important for developing optimal strategies to combat cancer [26]. Acetyl lysine marks on histones are most commonly recognized by small protein modules termed bromodomains (BrDs). Given the association of BrD-containing proteins with tumorigenesis [27], BrDs have become novel targets for cancer therapy [28]. The function of the YEATS domain as a histone acetylation reader has only been recently described. It has been shown that the YEATS domains of AF9 and ENL recognize acetylation on H3K9, H3K18 and H3K27, whereas that of YEATS2 preferentially binds to H3K27ac [24, 29, 30]. H2A.Z has been found to be overexpressed in a number of malignancies including bladder cancer, liver cancer and melanoma, and to play an oncogenic role in these tumors by regulating an enriched set of genes involved in cell cycle regulation and/or epithelial-mesenchymal transition [17, 31, 32]. The YEATS domain of GAS41 has been shown to recognize acetylation on H3K27 and H3K14 to promote H2A.Z deposition and, thereby, drive tumorigenesis of NSCLC [20]. However, whether GAS41 can read acetylation on H2A.Z is unknown.

In this study, we found that H2A.Z.2 is overexpressed in human pancreatic cancer tissues and cell lines. Exogenous expression of GAS41 or H2A.Z.2 upregulated NOTCH and NOTCH-mediated cancer cell stemness and *GEM* resistance. As GAS41 has previously been shown to promote H2A.Z deposition via histone acetylation [20], our findings directly link GAS41 and H2A.Z.2 to the chemoresistance of pancreatic cancer, a major cause of its poor prognosis. Thus, we hypothesized that GAS41 mediates H2A.Z.2 deposition and acetylation at the NOTCH locus

leading to increased Notch expression and activation. Concordantly, our co-IP experiments revealed a direct binding between GAS41 and H2A.Z.2 in pancreatic cancer cells, whereas this interaction was lost after the addition of a histone deacetylase. To the best of our knowledge, this is the first report of a YEATS domain protein acting as an acetylation reader for a histone or histone variant other than histone H3. In agreement with this notion, we found by ChIP that GAS41 overexpression promoted the deposition of H2A.Z.2 (presumably in its acetylated form) onto the promoter of NOTCH. This resulted in the activation of NOTCH and the expression of genes related to cancer cell stemness and drug resistance, leading to *GEM* resistance both *in vitro* and in an *in vivo* xenograft mouse model. GAS41 or H2A.Z.2 silencing deactivated NOTCH and sensitized pancreatic cancer cells to *GEM* *in vitro* and *in vivo*. Collectively, these findings indicate that blockade of the acetylation recognition activity between GAS41 and acH2A.Z.2 affects NOTCH activation and may help to combat pancreatic cancer chemoresistance and improve patient survival.

We also found that GAS41 was overexpressed in human pancreatic cancer tissues and cell lines. In addition, we found that a high GAS41 expression in human pancreatic cancer tissues was associated with a poor patient survival. Thus, GAS41 could potentially serve as a diagnostic and/or prognostic marker for pancreatic cancer. Previous studies have shown that GAS41 may be amplified in a variety of human cancers such as glioblastoma, stomach cancer and NSCLC [20, 33]. As yet, however, the functional role of GAS41 in cancer remains poorly defined. In the present study we identified the GAS41/acH2A.Z.2/NOTCH signaling cascade as a critical denominator in pancreatic cancer chemoresistance. Whether this pathway is also responsible for chemoresistance of other types of human cancer requires further investigation.

Our findings suggest that GAS41 can directly interact with acetylated H2A.Z, thereby promoting its deposition at the NOTCH promoter and increasing the expression and activation of the NOTCH pathway, linking GAS41/H2A.Z and NOTCH [15, 18, 19]. However, several important questions remain. For example, what is the mechanism by which GAS41 promotes the deposition of acH2A.Z.2. In addition, there are several limitations to our study. Our results indicated, for example, that GAS41 can promote pancreatic cancer cell proliferation in the absence of *GEM* treatment, suggesting that the increased proliferation may be due to increased resistance to *GEM* therapy induced by GAS41. However, it is also possible that the effect of GAS41 on promoting resistance to *GEM* treatment may be attributed at least partially to a general promotion of cellular proliferation. Future studies using GAS41 knockout cells may address this issue.

5 Conclusions

In summary, we found that overexpression of GAS41 in pancreatic cancer is involved in promoting cell proliferation and resistance to *GEM* through binding to acetylated H2A.Z and increased H2A.Z deposition, which leads to up-regulation of NOTCH. Thus, GAS41 may serve as a therapeutic target for overcoming chemoresistance of this malignancy.

Abbreviations *GEM*: Gemcitabine; CSCs: Cancer stem cells; GAS41: Glioma amplified sequence 41; GR: *GEM*-resistant; BrDs: Bromodomains; ChIP: Chromatin immunoprecipitation; NSCLC: non-small cell lung cancer

Supplementary Information The online version contains supplementary material available at <https://doi.org/10.1007/s13402-022-00675-8>.

Acknowledgements The authors are grateful for the support provided by the Tongji University School of Medicine and Shanghai Tenth People's Hospital.

Authors' contributions Shilong Han, Chuanwu Cao, Rui Liu: Conceptualization, Methodology, Software; Maoquan Li and Xiaoping Zhang: Supervision, Project administration; Shilong Han, Chuanwu Cao, Rui Liu: Data curation, Writing-Original draft preparation, Investigation; Yifeng Yuan, Long Pan, Minjie Xu, Chao Hu, Xiaojun Chao: Software, Validation. Maoquan Li and Xiaoping Zhang: Writing-Reviewing and Editing, Funding acquisition.

Funding This study was supported by the National Natural Science Foundation of China (No. 81801805), the Shanghai Sailing Program (No.16YF1409000) and the Climbing Talent Program of Shanghai Tenth People's Hospital (No. 2021SYPDRC014).

Data availability The datasets supporting the conclusions of this article are included in the article (and its additional files 1 to 17: Supplementary Material).

Declarations

Ethical approval and consent to participate All participating patients provided written informed consent and the human studies were approved by the Institute Research Ethics Committee of Shanghai Tenth People's Hospital. The study methodologies conformed to the standards set by the Declaration of Helsinki. The animal studies were performed in accordance with ARRIVE guidelines and were approved by the Institute Research Ethics Committee of the Shanghai Tenth People's Hospital.

Consent for publication Not applicable.

Competing interests The authors declare that they have no competing interests.

References

1. P. Rawla, T. Sunkara, V. Gaduputi, Epidemiology of Pancreatic Cancer: Global Trends, Etiology and Risk Factors. *World J Oncol.* **10**, 10–27 (2019)
2. F. Bray, J. Ferlay, I. Soerjomataram, R.L. Siegel, L.A. Torre, A. Jemal, Global cancer statistics 2018: GLOBOCAN estimates of incidence and mortality worldwide for 36 cancers in 185 countries. *CA Cancer J Clin.* **68**, 394–424 (2018)
3. R.L. Siegel, K.D. Miller, H.E. Fuchs, A. Jemal, Cancer Statistics, 2021. *CA: A Cancer Journal for Clinicians.* **71** (2021)
4. M. Manrai, T. Tilak, S. Dawra, S. Srivastava, A. Singh, Current and emerging therapeutic strategies in pancreatic cancer: Challenges and opportunities. *World J. Gastroenterol.* **27**, 6572–6589 (2021)
5. M.P. Kim, G.E. Gallick, Gemcitabine resistance in pancreatic cancer: picking the key players. *Clin Cancer Res.* **14**, 1284–1285 (2008)
6. A. Jain, V. Bhardwaj, Therapeutic resistance in pancreatic ductal adenocarcinoma: Current challenges and future opportunities. *World J. Gastroenterol.* **27**, 6527–6550 (2021)
7. B. Cpa, A. Bf, C. Bba, B. Dc, D. Gjpa, B. Pd, E. Yga, F. Ega, GSK3 β as a novel promising target to overcome chemoresistance in pancreatic cancer. *Drug Resistance Updates.* **58**, 100779 (2021)
8. A. Bvksl, B. Bf, C. Sl, D. Sp, E. Nsy, F. Pvb, I. Makgh, J. Mss, B. Gpn, Small molecule tyrosine kinase inhibitors and pancreatic cancer—Trials and troubles. *Seminars in Cancer Biology.* **54**, 149–167 (2019)
9. S.R. Martins-Neves, A.M. Cleton-Jansen, C.M.F. Gomes, Therapy-induced enrichment of cancer stem-like cells in solid human tumors: Where do we stand? *Pharmacol Res.* **137**, 193–204 (2018)
10. S. Chatterjee, P.C. Sil, Targeting the crosstalks of Wnt pathway with Hedgehog and Notch for cancer therapy. *Pharmacol Res.* **142**, 251–261 (2019)
11. V. Venkatesh, R. Nataraj, G.S. Thangaraj, M. Karthikeyan, A. Gnanasekaran, S.B. Kaginelli, G. Kuppanna, C.G. Kallappa, K.M. Basalingappa, Targeting Notch signalling pathway of cancer stem cells. *Stem Cell Investig.* **5**, 5 (2018)
12. Z. Wang, Y. Li, D. Kong, S. Banerjee, A. Ahmad, A.S. Azmi, S. Ali, J.L. Abbruzzese, G.E. Gallick, F.H. Sarkar, Acquisition of epithelial-mesenchymal transition phenotype of gemcitabine-resistant pancreatic cancer cells is linked with activation of the notch signaling pathway. *Cancer Res.* **69**, 2400–2407 (2009)
13. B.D. Giaimo, F. Ferrante, A. Herchenrother, S.B. Hake, T. Borggreffe, The histone variant H2A.Z in gene regulation. *Epigenetics Chromatin.* **12**, 37 (2019)
14. D. Corujo, M. Buschbeck, Post-Translational Modifications of H2A Histone Variants and Their Role in Cancer. *Cancers (Basel).* **10** (2018)
15. B.D. Giaimo, F. Ferrante, D.M. Vallejo, K. Hein, I. Gutierrez-Perez, A. Nist, T. Stiewe, G. Mittler, S. Herold, T. Zimmermann, M. Bartkuhn, P. Schwarz, F. Oswald, M. Dominguez, T. Borggreffe, Histone variant H2A.Z deposition and acetylation directs the canonical Notch signaling response. *Nucleic Acids Res.* **46**, 8197–8215 (2018)
16. J.M. Eirin-Lopez, R. Gonzalez-Romero, D. Dryhurst, T. Ishibashi, J. Ausio, The evolutionary differentiation of two histone H2A.Z variants in chordates (H2A.Z-1 and H2A.Z-2) is mediated by a stepwise mutation process that affects three amino acid residues. *BMC Evol Biol.* **9**, 31 (2009)
17. C. Vardabasso, A. Gaspar-Maia, D. Hasson, S. Punzeler, D. Valle-Garcia, T. Straub, E.C. Keilhauer, T. Strub, J. Dong, T. Panda, C.Y. Chung, J.L. Yao, R. Singh, M.F. Segura, B. Fontanalas-Cirera, A. Verma, M. Mann, E. Hernando, S.B. Hake, E. Bernstein, Histone Variant H2A.Z.2 Mediates Proliferation and Drug Sensitivity of Malignant Melanoma. *Mol Cell.* **59**, 75–88 (2015)
18. M.M. Wong, L.K. Cox, J.C. Chrivia, The chromatin remodeling protein, SRCAP, is critical for deposition of the histone variant H2A.Z at promoters. *J Biol Chem.* **282**, 26132–26139 (2007)
19. A. Cuadrado, N. Corrado, E. Perdiguero, V. Lafarga, P. Munoz-Canoves, A.R. Nebreda, Essential role of p18Hamlet/SRCAP-mediated histone H2A.Z chromatin incorporation in muscle differentiation. *EMBO J.* **29**, 2014–2025 (2010)

20. C.C. Hsu, J. Shi, C. Yuan, D. Zhao, S. Jiang, J. Lyu, X. Wang, H. Li, H. Wen, W. Li, X. Shi, Recognition of histone acetylation by the GAS41 YEATS domain promotes H2A.Z deposition in non-small cell lung cancer. *Genes Dev.* **32**, 58–69 (2018)
21. D.G. Berta, H. Kuisma, N. Vlimki, M. Risnen, L.A. Aaltonen, Deficient H2A.Z deposition is associated with genesis of uterine leiomyoma. *Nature.* **596**, 398–403 (2021)
22. G.M. Christman, H. Tang, I. Ahmad, J.M. Stribley, Differential expression of the Notch signal transduction pathway: ligands, receptors and Numb in uterine leiomyomas vs. myometrium. *Fertility & Sterility.* **88**, S72–S72 (2007)
23. X. Hu, P. Chen, Y. Wu, K. Wang, Y. Xu, H. Chen, L. Zhang, R. Wu, K.A. Webster, H. Yu, W. Zhu, J. Wang, MiR-211/STAT5A Signaling Modulates Migration of Mesenchymal Stem Cells to Improve its Therapeutic Efficacy. *Stem Cells.* **34**, 1846–1858 (2016)
24. Y. Li, H. Wen, Y. Xi, K. Tanaka, H. Wang, D. Peng, Y. Ren, Q. Jin, S.Y. Dent, W. Li, H. Li, X. Shi, AF9 YEATS domain links histone acetylation to DOT1L-mediated H3K79 methylation. *Cell.* **159**, 558–571 (2014)
25. Z.H. Liu, X.M. Dai, B. Du, Hes1: a key role in stemness, metastasis and multidrug resistance. *Cancer Biol Ther.* **16**, 353–359 (2015)
26. C.B. Benton, W. Fiskus, K.N. Bhalla, Targeting Histone Acetylation: Readers and Writers in Leukemia and Cancer. *Cancer J.* **23**, 286–291 (2017)
27. T. Fujisawa, P. Filippakopoulos, Functions of bromodomain-containing proteins and their roles in homeostasis and cancer. *Nat Rev Mol Cell Biol.* **18**, 246–262 (2017)
28. J. Qi, Bromodomain and extraterminal domain inhibitors (BETi) for cancer therapy: chemical modulation of chromatin structure. *Cold Spring Harb Perspect Biol.* **6**, a018663 (2014)
29. D. Zhao, H. Guan, S. Zhao, W. Mi, H. Wen, Y. Li, Y. Zhao, C.D. Allis, X. Shi, H. Li, YEATS2 is a selective histone crotonylation reader. *Cell Res.* **26**, 629–632 (2016)
30. L. Wan, H. Wen, Y. Li, J. Lyu, Y. Xi, T. Hoshii, J.K. Joseph, X. Wang, Y.E. Loh, M.A. Erb, A.L. Souza, J.E. Bradner, L. Shen, W. Li, H. Li, C.D. Allis, S.A. Armstrong, X. Shi, ENL links histone acetylation to oncogenic gene expression in acute myeloid leukaemia. *Nature.* **543**, 265–269 (2017)
31. K. Kim, V. Punj, J. Choi, K. Heo, J.M. Kim, P.W. Laird, W. An, Gene dysregulation by histone variant H2A.Z in bladder cancer. *Epigenetics Chromatin.* **6**, 34 (2013)
32. H.D. Yang, P.J. Kim, J.W. Eun, Q. Shen, H.S. Kim, W.C. Shin, Y.M. Ahn, W.S. Park, J.Y. Lee, S.W. Nam, Oncogenic potential of histone-variant H2A.Z.1 and its regulatory role in cell cycle and epithelial-mesenchymal transition in liver cancer. *Oncotarget.* **7**, 11412–11423 (2016)
33. U. Fischer, D. Heckel, A. Michel, M. Janka, T. Hulsebos, E. Meese, Cloning of a novel transcription factor-like gene amplified in human glioma including astrocytoma grade I. *Hum Mol Genet.* **6**, 1817–1822 (1997)

Publisher's note Springer Nature remains neutral with regard to jurisdictional claims in published maps and institutional affiliations.